18

Investigation of the stability of the optical characteristics of thin films based on $CsPbBr_3$ perovskite nanocrystals and p(MMA-LMA) copolymer

© A.A. Knysh[1], D.G. Gulevich[1], I.R. Nabiev[2,3], P.S. Samokhvalov[1,2,¶]

[1] Laboratory of Nanobioengineering, National Research Nuclear University MEPhI (Moscow Engineering Physics Institute), 115409 Moscow, Russia
[2] LIFT Center, Skolkovo, 121205 Moscow, Russia
[3] Laboratoire de Recherche en Nanosciences (LRN-EA4682), Université de Reims Champagne-Ardenne, 51100 Reims, France

¶ e-mail: p.samokhvalov@gmail.com

Received September 22, 2023
Revised September 22, 2023
Accepted September 28, 2023

Despite the excellent optical characteristics of perovskite nanocrystals (PNCs) based on $CsPbBr_3$, they have a relatively low stability, which limits their use as materials for hybrid light-emitting diodes, single-photon sources, solar cells, and other optoelectronic devices, as well as X-ray and gamma-ray detectors. The present study reports the results of experiments on composite thin films based on PNCs and copolymer of methyl and lauryl methacrylates. The changes in the quantum yield and mean luminescence lifetime in thin film samples with different copolymer mass fractions relative to $CsPbBr_3$-based PNCs have been investigated. It has been shown that composite samples containing from 10 to 20 wt.% of copolymer have an improved temporal stability of optical characteristics, which makes them promising for practical use in optoelectronic applications.

Keywords: perovskite nanocrystals, thin films, luminescence kinetics, quantum yield.

DOI: 10.61011/EOS.2023.09.57350.5588-23

Introduction

Nanocrystals (NCs) based on cesium lead halides with a general formula of $CsPbX_3$ (X is a halide anion) and a perovskite structure rank among the most promising types of colloidal NCs. An upsurge in interest in a wide range of potential applications of perovskite nanocrystals (PNCs) in optoelectronics has been noted in recent years (specifically, since 2015 [1]). Although this promising class of nanomaterials is being studied extensively, the problem of long-term structural and optical stability of PNCs still remains unsolved. External factors such as light, moisture, and air oxygen are the ones that normally cause PNC degradation in the course of long-term operation [2,3]. Cesium lead bromide perovksites are considered to be the most stable of $CsPbX_3$ PNCs [4], but even they are still insufficiently stable for commercial applications. Several approaches to solving this problem, which include PNC doping by partial substitution of cesium or lead cations [5,6], chemical modification of the PNC surface via ligand exchange [7,8], and NC encapsulation in inorganic [9,10] and organic [11–14] shells/matrices, have been proposed. The last of the mentioned approaches is particularly promising in the context of PNC application to X-ray imaging [13,15].

Considerable advances in the fabrication of composites based on $CsPbBr_3$ and polymers of various compositions, which provide, to some extent, a solution to the PNC stability problem, have already been made. Specifically, Xin et. al [16] have reported an enhancement of photoluminescence intensity and retention of optical characteristics of composites $CsPbBr_3$ PNCs with polymethyl methacrylate (PMMA) and polybutyl methacrylate (PBMA) synthesized via UV polymerization. It turned out that PNC-PMMA and PNC-PBMA samples retained 70 and 78% of PL intensity for 30 days of exposure to air and 54 and 56% of PL intensity for 48 h of exposure to water. The encapsulation of $CsPbBr_3$ PNCs in a polystyrene (PS) matrix enhanced the resistance of PNCs to moisture, providing the possibility to retain 65% of photoluminescence intensity during 3 days of measurements (and up to 69% of photoluminescence intensity for samples processed in an alkali solution with pH 11) [17]. Li et al. [12] have demonstrated that the copolymer of ethylene and vinyl acetate is highly efficient in obtaining composite thin films, with their optical properties remaining unchanged even after 1000 successive cycles of mechanical bending and 8 and 10 days of exposure to air and water, respectively. In addition, it turned out that the *in situ* crystallization strategy for growth of $CsPbBr_3$ NCs in poly(vinylidene difluoride) yields composite samples with high thermal stability, which helps preserve a constant quantum yield upon heating to 170°C [14]. Using spray-drying encapsulation in the process of fabrication of composite films, Boussoufi et al. [18] have obtained PNC-PMMA and PNC-PBMA composites resistant to light and high tempera-

tures. Notably, composites of $CsPbBr_3$ with polyaniline [11]; polyvinylpyrollidone [19]; poly(isopropyl methacrylate) [20] (a copolymer of ethylene and norbornene); and block copolymers of styrene, ethylene, and butylene [21] have also exhibited improved long-term optical performance.

In the present study, the destructive effect of the environment is mitigated by encapsulation of PNCs in a polymer matrix based on a copolymer of MMA and lauryl methacrylate (LMA) obtained using free radical polymerization. The proposed approach is promising in terms of establishing an efficient protection of PNCs not only from ambient effects, but also from penetrating luminescence-quenching molecules, contributing to the long-term stability of a composite luminescent material. The polymer matrix composition was chosen due to a high optical transparency and hydrophobic properties of the copolymer. The temporal variations of the luminescence intensity and the quantum yield of PL of the obtained samples were in order to analyze the optical properties of thin PNC–p(MMA-LMA) films and determine the optimum copolymer content and temperature regime of film synthesis.

Materials and methods

Colloidal $CsPbBr_3$ PNCs were synthesized using the injection method in a nonpolar medium with cesium oleate and lead bromide precursors in accordance with the procedure described by Protesescu et al. [22]. The synthesis was discussed in detail in our previous study [23]. The concentration of PNCs in the initial solution was 20 mg/ml. $CsPbBr_3$ samples were treated with argon and stored at room temperature with no exposure to light. Matrices based on a copolymer of methyl- and lauryl methacrylates (at a ratio of 2:1) were synthesized by radical polymerization in an inert atmosphere at a temperature of 95°C with 1,1′-azobis(cyclohexanecarbonitrile) used as an initiator [24].

Thin films of the composite of $CsPbBr_3$ PNCs and the p(MMA-LMA) copolymer were deposited onto glass substrates that were preliminarily cleaned. This cleaning involved a long-term treatment of the substrates with a mixture of concentrated sulfuric acid (H_2SO_4) and potassium dichromate ($K_2Cr_2O_7$) and a mixture of concentrated nitric (HNO_3) and hydrochloric (HCl) acids (at a volume ratio of 1:3) and intermediate rinsing with tap and deionized water. Glass substrates were then dried in a drying cabinet at a temperature of 110°C for 2 h.

Composite thin films (TFs) were fabricated by spin coating [25] using a Spin-Coater KW-4A setup (Chemat). The films were formed by depositing 100 μl of a solution of PNCs and the p(MMA-LMA) copolymer onto glass substrates. The weight fraction of the p(MMA-LMA) was varied from 0 to 90% relative to the percentage of $CsPbBr_3$ in octane. The optimum rotation rate and duration were determined to be 2000 rpm and 60 s, respectively. Part of the samples were then annealed at 100°C for 5 min to estimate the influence of temperature on the structural and optical properties of the TFs.

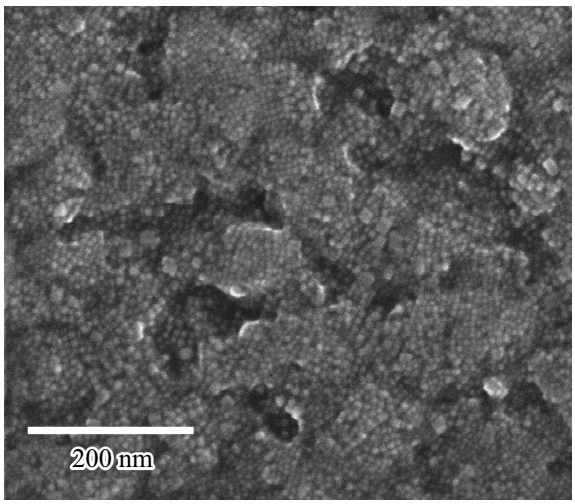

Figure 1. SEM images of a thin film based on $CsPbBr_3$ PNCs.

The TF surface microstructure was examined by scanning electron microscopy (SEM) with a JEOL7900F microscope at an accelerating voltage of 30 kV.

The photoluminescence (PL) kinetics of the composite TF samples was measured at intervals of four days. The obtained experimental data were approximated by the function $I(t)$ (the PL variation law was considered to be bi-exponential [26]):

$$I(t) = I_0 + Q_1 e^{-\frac{t}{\tau_1}} + Q_2 e^{-\frac{t}{\tau_2}}, \quad (1)$$

where $I(t)$ is the PL intensity, I_0 is a constant, t is the decay time, Q_1 and Q_2 are the pre-exponential factors of the approximation function, and τ_1 and τ_2 are the time constants of the fast and slow PL decay components, respectively.

The average luminescence lifetime (τ_{av}) was calculated [27] using the following equation

$$\tau_{av} = \sum_{i=1}^{p} Q_i \tau_i^2 / \sum_{i=1}^{p} Q_i \tau_i, \quad (2)$$

where p is the number of PL decay components.

Results and discussion

Samples of the composite TFs based on PNCs and the p(MMA-LMA) copolymer with a weight contents of 0, 2, 10, 20, 50, and 90% relative to $CsPbBr_3$ were fabricated by spin coating. The results of SEM imaging (Fig. 1) suggest that the TFs obtained under the specified experimental conditions provided a fairly uniform PNC coverage of the substrate. It seems likely that local porous structures formed in the course of evaporation of the solvent. Figure 2 presents the PL decay curves for the fabricated TFs measured

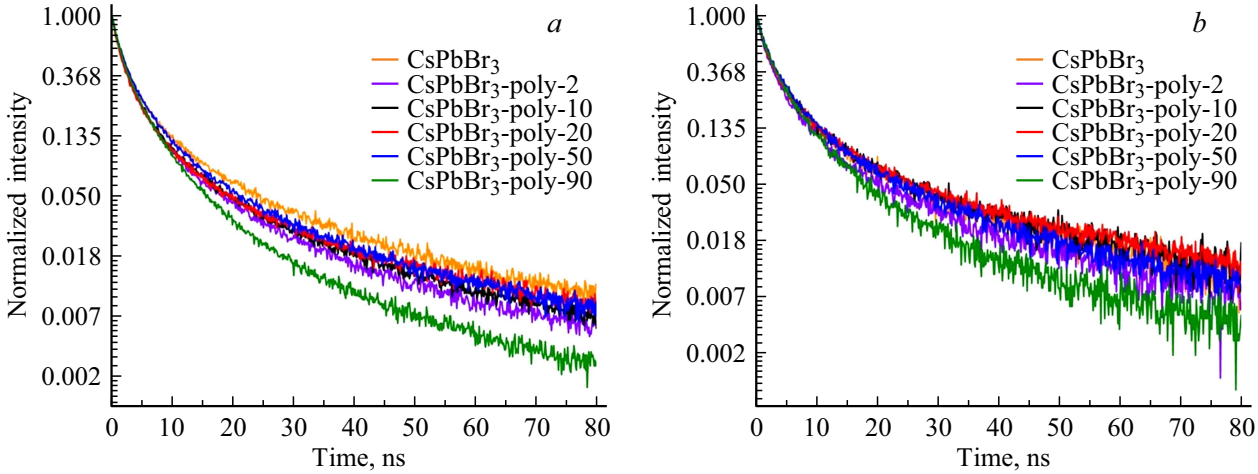

Figure 2. PL decay curves for $CsPbBr_3$, $CsPbBr_3$-poly-2, $CsPbBr_3$-poly-10, $CsPbBr_3$-poly-20, $CsPbBr_3$-poly-50, and $CsPbBr_3$-poly-90 TF samples measured on the first day (*a*) and on the fifth day (*b*) after synthesis.

Average PL lifetimes for TFs based on $CsPbBr_3$ PNCs and the p(MMA-LMA) copolymer

TF sample	Weight fraction of p(MMA-LMA), %	τ_1, ns (first day)	τ_2, ns (first day)	τ_1, ns (fifth day)	τ_2, ns (fifth day)	τ_{av}, ns (first day)	τ_{av}, ns (fifth day)
$CsPbBr_3$	0	2.1	17.0	2.1	16.5	12.6 ± 0.3	12.2 ± 0.3
$CsPbBr_3$-poly-2	2	2.1	13.7	2.1	14.7	9.4 ± 0.2	10.6 ± 0.3
$CsPbBr_3$-poly-10	10	2.0	14.5	2.4	19.1	10.1 ± 0.2	13.7 ± 0.4
$CsPbBr_3$-poly-20	20	2.0	15.4	2.3	19.8	10.8 ± 0.3	14.3 ± 0.4
$CsPbBr_3$-poly-50	50	2.3	15.6	2.4	16.2	10.9 ± 0.2	11.7 ± 0.3
$CsPbBr_3$-poly-90	90	2.0	9.6	2.2	10.7	6.9 ± 0.1	7.9 ± 0.2

immediately after the deposition of films onto substrates and on the fifth day after fabrication.

The average PL lifetime was calculated for the synthesized samples from the obtained experimental data (see the table). As seen from the table, the average PL lifetime of the synthesized TFs varies nonmonotonically with increasing copolymer concentration. Specifically, the lowest τ_{av} value corresponds to the composite TF sample with the highest copolymer concentration (90%); at other concentrations the average PL lifetime increases in the following order $CsPbBr_3$-poly-2, $CsPbBr_3$-poly-20, $CsPbBr_3$-poly-50, and pure $CsPbBr_3$ (see Fig. 2, *a* and the table). The PL kinetics curves for $CsPbBr_3$-poly-20 and $CsPbBr_3$-poly-50 are identical in shape, which is evidenced by their τ_{av} (see the table). The measurements of PL kinetics on the fifth day (see Fig. 2, *b* and the table) revealed a similar trend; the sole exception was the $CsPbBr_3$-poly-20 sample with the maximum τ_{av} value. The calculated average PL lifetimes for composite samples are within the margins of error; in the case of pure $CsPbBr_3$ PNC TFs, they agree with literature data [28]. The enhancement of τ_{av} on the fifth day of observations, which is especially pronounced in the case of $CsPbBr_3$-poly-20 TFs, is likely to be related to stress relaxation and the removal of molecular oxygen (MO), which is the main PL quenching agent [29] and is contained within freshly formed composite samples.

The deviation of the bi-exponential approximation from the theoretical mono-exponential law is indicative of the presence of aggregates and a nonuniform distribution of NCs in the TF layer. This offers the opportunity to isolate regions emitting photons with different characteristic times within the bulk composite. Specifically, PL quenching processes may be induced by nonradiative carrier recombination and the dipole–dipole Förster resonance energy transfer (FRET) [30].

The observed enhancement of the average PL lifetime on the fifth day of measurements can also be attributed to a change in the degree of aggregation of $CsPbBr_3$ PNCs in the samples. This process is apparently influenced by the polymer matrix structure, which is determined by the p(MMA-LMA) concentration. The results of approximation of experimental PL decay curves (see the table) have

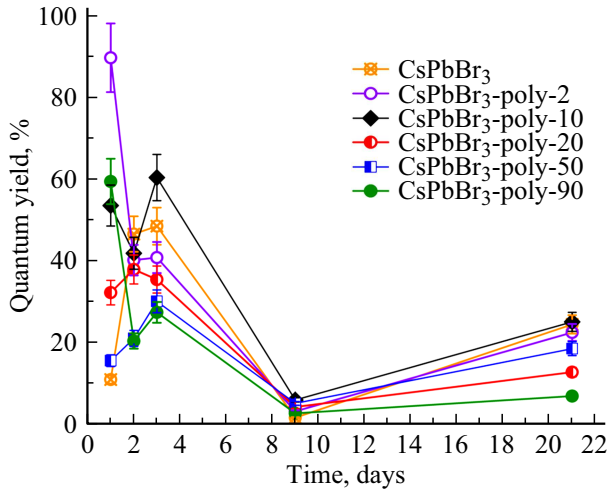

Figure 3. Time course of the variation of PL QY for the $CsPbBr_3$, $CsPbBr_3$-poly-2, $CsPbBr_3$-poly-10, $CsPbBr_3$-poly-20, $CsPbBr_3$-poly-50, and $CsPbBr_3$-poly-90 samples stored under normal conditions.

shown that the contribution of the long-lived component of luminescence kinetics of the synthesized TF samples increases with time, indicating an increase in the proportion of individual PNCs in the bulk composite. This is related to the presence of LMA fragments, which are more compatible with the PNC surface, in the polymer matrix.

Alongside with kinetics measurements, the quantum yield (QY) of PL of the thin films was monitored for 20 days. A drastic PL QY reduction followed by a gradual increase, was observed at the start of measurements (Fig. 3). This initial QY reduction is likely have been related to transient processes in the bulk TFs and the influence of MO. The QY enhancement in the course of long-term storage can be attributed to further reduction of the MO concentration in the bulk TFs. Since equilibrium is established in the TF in the course of time due to irregular loss of MO from the synthesized samples, the QY values are likely to fluctuate (Fig. 3). According to the results of 20 days of QY measurements, the strongest stabilizing effect was observed in the composite sample with a p(MMA-LMA) copolymer weight fraction of 20%.

The data presented in Fig. 3 suggest that the PL QY decreases with time as the copolymer weight fraction in the composite increases. This is apparently attributable to the fact that a p(MMA-LMA) copolymer excess facilitates the segregation of the PNC and copolymer phases, contributing to a relative increase in the proportion of PNCs in the aggregated state.

In order to verify the proposed hypothesis regarding composite stabilization by LMA fragments present in the polymer, composite TF samples with low copolymer concentrations were fabricated additionally. Immediately after synthesis, these samples were annealed at a temperature of 100°C for 5 min. The presumed dissociation of aggregates should then occur in the course of annealing. It was found experimentally that thermal treatment had no significant influence on the PL QY. However, the average PL lifetime of the annealed samples increased, which indicated that transient processes ceased (and MO escaped from the bulk of TFs) rapidly. Figure 4 presents a comparison between the variations of the average PL lifetime for a TF of pure PNCs and a composite TF with a copolymer weight fraction of 10 % ($CsPbBr_3$-poly-10) with time. It can be seen that the film annealing procedure is indeed efficient in terms of acceleration of relaxation processes in composites. It should be noted that thermal processing of the films did not improve the optical parameters of samples with a copolymer weight fraction in the composite above 50%.

Since the results of our experiments demonstrated that τ_{av} increased with time, it was reasonable to expect that the QY of PL of the studied samples would increase simultaneously. However, this was not observed. This discrepancy can be attributed to the physical nature of PNCs, which are similar to well-known chalcogenide quantum dots (QDs). Charge transfer processes, which induce variations of PL QY values over time [32], are typical of such QDs [31]. Two groups of PNCs may be isolated in the NC ensemble in the bulk of synthesized samples: „switched-off" crystals, which only absorb radiation in a wide band, the excitation within which being relaxed via nonradiative processes, and „switched-on" PNCs, which absorb light and reradiate it. Emitting PNCs can be further divided into two classes corresponding to the fast and slow PL kinetics components: PNCs in the normal „switched-on" state and „gray" PNCs carrying an additional charge [32], respectively. When samples are subjected to prolonged irradiation (e.g., in the course of measurements), the percentage of „switched-off" NCs in the nanoparticle ensemble may increase due to photoinduced transfer of electrons to the bulk polymer matrix, inducing a PL QY reduction but having no effect

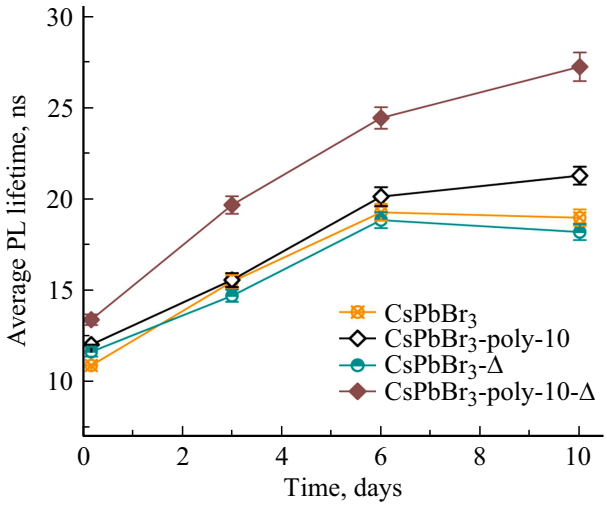

Figure 4. Time course of the variation of average PL lifetimes of $CsPbBr_3$ and $CsPbBr_3$-poly-10 TF samples in comparison with the samples subjected to thermal processing ($CsPbBr_3$-Δ and $CsPbBr_3$-poly-10-Δ).

on the PL decay kinetics. At the same time, as part of PNCs is being „switched off," the initially charged „gray" NCs become neutralized, which leads to an increase in the percentage of NCs with the slow kinetics component and, consequently, to an increase in τ_{av}, as illustrated in Fig. 4. It is worth noting in conclusion that the processes described above may provide an explanation for the discrepancy between an increasing τ_{av} and a simultaneously decreasing PL QY.

Conclusion

Composite TF samples based on $CsPbBr_3$ PNCs and the p(MMA-LMA) copolymer whose fraction varies from 0 to 90% relative to the PNCs were synthesized by spin coating. Long-term measurements of PL kinetics revealed a complex nature of dependence of the TF optical properties on the PNC-to-polymer ratio. The average PL lifetime and luminescence QY values were determined. The parameters of the TF sample containing 20% of p(MMA-LMA) were found to be the most stable in the course of long-term storage. The variation of optical characteristics of samples in kinetics measurements performed on the first day after film synthesis is apparently attributable to FRET quenching of luminescence in aggregates and to the presence of MO (with its concentration decreasing with time due to gradual loss) in the bulk composite. It has been demonstrated that the procedure of thermal TF treatment does not improve the optical parameters of composite samples with a high copolymer weight fraction, although the average PL lifetime does increase considerably after annealing in composites containing less than 50% of p(MMA-LMA). The obtained results suggest good prospects for composite nanomaterials to be used as a light-emitting active layer of advanced hybrid LEDs and an activating scintillation layer in medical X-ray detectors.

Funding

This study was supported by the Ministry of Science and Higher Education of the Russian Federation, grant No. 075-15-2021-1413.

Conflict of interest

The authors declare that they have no conflict of interest.

References

[1] Q.A. Akkerman, G. Rainó, M.V. Kovalenko, L. Manna. Nat. Mater., **17** (5), 394–405 (2018). DOI: 10.1038/s41563-018-0018-4
[2] D. Wang, M. Wright, N.K. Elumalai, A. Uddin. Sol. Energy Mater. Sol. Cells., **147**, 255–275 (2016). DOI: 10.1016/j.solmat.2015.12.025
[3] A.H. Slavney, R.W. Smaha, I.C. Smith, A. Jaffe, D. Umeyama, H.I. Karunadasa. Inorg. Chem., **56**(1), 46–55 (2017). DOI: 10.1021/acs.inorgchem.6b01336
[4] Q. Sun, W.-J.Yin. J. Am. Chem. Soc., **139** (42), 14905–14908 (2017). DOI: 10.1021/jacs.7b09379
[5] Z.-J. Yong, S.-Q. Guo, J.-P. Ma, J.-Y. Zhang, Z.-Y. Li, Y.-M. Chen, B.-B. Zhang, Y. Zhou, J. Shu, J.-L. Gu, L.-R. Zheng, O.M. Bakr, H.-T. Sun. J. Am. Chem. Soc., **140** (31), 9942–9951 (2018). DOI: 10.1021/jacs.8b04763
[6] G.H. Ahmed, Y. Liu, I. Bravić, X. Ng, I. Heckelmann, P. Narayanan, M.S. Fernández, B. Monserrat, D.N. Congreve, S. Feldmann. J. Am. Chem. Soc., **144**(34), 15862–15870 (2022). DOI: 10.1021/jacs.2c07111
[7] F. Wang, W. Geng, Y. Zhou, H.-H. Fang, C.-J. Tong, M.A. Loi, L.-M. mLiu, N. Zhao. Adv. Mater., **28** (45), 9986–9992 (2016). DOI: 10.1002/adma.201603062
[8] J. De Roo, M. Ibáñez, P. Geiregat, G. Nedelcu, W. Walravens, J. Maes, J.C. Martins, I. Van Driessche, M.V. Kovalenko, Z. Hens. ACS Nano, **10** (2), 2071–2081 (2016). DOI: 10.1021/acsnano.5b06295
[9] H.C. Yoon, S. Lee, J.K. Song, H. Yang, Y.R. Do. ACS Appl. Mater. Interfaces, **10** (14), 11756–11767 (2018). DOI: 10.1021/acsami.8b01014
[10] H. Hu, L. Wu, Y. Tan, Q. Zhong, M. Chen, Y. Qiu, D. Yang, B. Sun, Q. Zhang, Y. Yin. J. Am. Chem. Soc., **140** (1), 406–412 (2018). DOI: 10.1021/jacs.7b11003
[11] Z. Zhang, L. Li, L. Liu, X. Xiao, H. Huang, J. Xu. J. Phys. Chem. C, **124** (40), 22228–22234 (2020). DOI: 10.1021/acs.jpcc.0c05774
[12] Y. Li, Y. Lv, Z. Guo, L. Dong, J. Zheng, C. Chai, N. Chen, Y. Lu, C. Chen. ACS Appl. Mater. Interfaces, **10**(18), 15888–15894 (2018). DOI: 10.1021/acsami.8b02857
[13] J. Nie, C. Li, S. Zhou, J. Huang, X. Ouyang, Q. Xu. ACS Appl. Mater. Interfaces, **13** (45), 54348–54353 (2021). DOI: 10.1021/acsami.1c15613
[14] P. Liang, P. Zhang, A. Pan, K. Yan, Y. Zhu, M. Yang, L. He. ACS Appl. Mater. Interfaces, **11** (25), 22786–22793 (2019). DOI: 10.1021/acsami.9b06811
[15] Y. Zhou, J. Chen, O.M. Bakr, O.F. Mohammed. ACS Energy Lett., **6**(2), 739–768 (2021). DOI: 10.1021/acsenergylett.0c02430
[16] Y. Xin, H. Zhao, J. Zhang. ACS Appl. Mater. Interfaces, **10** (5), 4971–4980 (2018). DOI: 10.1021/acsami.7b16442
[17] Y. Wei, X. Deng, Z. Xie, X. Cai, S. Liang, P. Ma, Z. Hou, Z. Cheng, J. Lin. Adv. Funct. Mater., **27** (39), 1703535 (2017). DOI: 10.1002/adfm.201703535
[18] F. Boussoufi, M. Pousthomis, A. Kuntzmann, M. D'Amico, G. Patriarche, B. Dubertret. ACS Appl. Nano Mater., **4** (7), 7502–7512 (2021). DOI: 10.1021/acsanm.1c01552
[19] T. Dong, J. Zhao, G. Li, F.-C. Li, Q. Li, S. Chen. ACS Appl. Mater. Interfaces, **13** (33), 39748–39754 (2021). DOI: 10.1021/acsami.1c10806
[20] T.A. Cohen, Y. Huang, N.A. Bricker, C.S. Juhl, T.J. Milstein, J.D. McKenzie, C.K. Luscombe, D.R. Gamelin. Chem. Mater., **33** (10), 3779–3790 (2021). DOI: 10.1021/acs.chemmater.1c00902
[21] G. Rainó, A. Landuyt, F. Krieg, C. Bernasconi, S.T. Ochsenbein, D.N. Dirin, M.I. Bodnarchuk, M.V. Kovalenko. Nano Lett., **19** (6), 3648–3653 (2019). DOI: 10.1021/acs.nanolett.9b00689

[22] L. Protesescu, S. Yakunin, M.I. Bodnarchuk, F. Krieg, R. Caputo, C.H. Hendon, R. X. Yang, A. Walsh, M.V. Kovalenko. Nano Lett., **15** (6), 3692–3696 (2015). DOI: 10.1021/nl5048779
[23] D.G. Gulevich, A.A. Tkach, I.R. Nabiev, V.A. Krivenkov, P.S. Samokhvalov. Tech. Phys., **68**(2), 241 (2023). DOI: 10.21883/TP.2023.02.55479.240-22
[24] A. Knysh, A. Tkach, D. Gulevich, I. Nabiev, P. Samokhvalov. Phys. At. Nucl., **85** (10), 1619–1624 (2022). DOI: 10.1134/S1063778822090186
[25] V. Chernikova, O. Shekhah, M. Eddaoudi. ACS Appl. Mater. Interfaces, **8** (31), 20459–20464 (2016). DOI: 10.1021/acsami.6b04701
[26] F. Zhang, H. Zhong, C. Chen, X. Wu, X. Hu, H. Huang, J. Han, B. Zou, Y. Dong. ACS Nano, **9** (4), 4533–4542 (2015). DOI: 10.1021/acsnano.5b01154
[27] Y. Li, S. Natakorn, Y. Chen, M. Safar, M. Cunningham, J. Tian, D.D.-U. Li. Front. Phys., **8** (2020). DOI: 10.3389/fphy.2020.576862
[28] X. Du, G. Wu, J. Cheng, H. Dang, K. Ma, Y.-W. Zhang, P.-F. Tan, S. Chen. RSC Adv., **7** (17), 10391–10396 (2017). DOI: 10.1039/C6RA27665B
[29] J.R. Lakowicz. *Principles of Fluorescence Spectroscopy* (Springer US: Boston, MA, 2006). DOI: 10.1007/978-0-387-46312-4
[30] R.M. Clegg. Curr. Opin. Biotechnol., **6** (1), 103–110 (1995). DOI: 10.1016/0958-1669(95)80016-6
[31] K.V. Vokhmintcev, P.S. Samokhvalov, I. Nabiev. Nano Today, **11** (2), 189–211 (2016). DOI: 10.1016/j.nantod.2016.04.005
[32] V. Krivenkov, P. Samokhvalov, M. Zvaigzne, I. Martynov, A. Chistyakov, I. Nabiev. J. Phys. Chem. C, **122** (27), 15761–15771 (2018). DOI: 10.1021/acs.jpcc.8b04544

Translated by D.Safin